Glycobiology, 2018, vol. 28, no. 1, 32–41
doi: 10.1093/glycob/cwx090
Advance Access Publication Date: 23 October 2017
Original Article

OXFORD

Cell Biology

Loss of heparan sulfate in the niche leads to tumor-like germ cell growth in the *Drosophila* testis

Daniel C Levings and Hiroshi Nakato*

Department of Genetics, Cell Biology and Development, The University of Minnesota, 6-160 Jackson Hall, 321 Church St SE, Minneapolis, MN 55455, USA

*To whom correspondence should be addressed: Tel: +1-612-625-1727; Fax: +1-612-626-5652; e-mail: nakat003@umn.edu

Received 3 August 2017; Revised 10 October 2017; Editorial decision 11 October 2017; Accepted 17 October 2017

Abstract

The stem cell niche normally prevents aberrant stem cell behaviors that lead to cancer formation. Recent studies suggest that some cancers are derived from endogenous populations of adult stem cells that have somehow escaped from normal control by the niche. However, the molecular mechanisms by which the niche retains stem cells locally and tightly controls their divisions are poorly understood. Here, we demonstrate that the presence of heparan sulfate (HS), a class glygosaminoglycan chains, in the *Drosophila* germline stem cell niche prevents tumor formation in the testis. Loss of HS in the niche, called the hub, led to gross changes in the morphology of testes as well as the formation of both somatic and germline tumors. This loss of hub HS resulted in ectopic signaling events in the Jak/Stat pathway outside the niche. This ectopic Jak/Stat signaling disrupted normal somatic cell differentiation, leading to the formation of tumors. Our finding indicates a novel non-autonomous role for niche HS in ensuring the integrity of the niche and preventing tumor formation.

Key words: *Drosophila*, germline stem cell niche, germline tumor, heparan sulfate, Jak-Stat signalling

Introduction

Stem cells typically reside in a specialized microenvironment termed "niche" which provides stem cells with signals necessary for their maintenance (Scadden 2006). Precise control of stem cell proliferation and the retention of stem cells to the niche are important to prevent cancer formation (Clarke and Fuller 2006). Recent studies have suggested that endogenous populations of adult stem cells can sometimes escape from normal control of the niche and become so-called cancer stem cells (CSCs) (Houghton et al. 2004; Clarke and Fuller 2006). Disrupted niche control could predispose a stem cell to such CSC transformation (Bhowmick et al. 2004; Radisky and Bissell 2004). It has been suggested that germ cell tumors can be caused by such malfunction of the germline stem cell niche (Gilbert et al. 2011). In the mammalian testis, the main niche component for spermatogonial stem cells (SSCs) is thought to be the somatic Sertoli cells (Hai et al. 2014). Sertoli cells enwrap the SSCs and undifferentiated spermatogonia and provide the GDNF signal, which is most critical for SSC renewal (Meng et al. 2000). Thus, it has been proposed that misregulation of this niche signaling can lead to testicular germ cell tumors, the most common malignancy in young men (Gilbert et al. 2011; Krausz and Looijenga 2008; Krentz et al. 2009). However, the mechanism by which dysregulation of stem cell niche signaling causes tumor formation remains to be elucidated.

The germline stem cell (GSC) niche in the *Drosophila* testis offers an excellent model to study the molecular mechanisms of stem cell maintenance and differentiation. Similar to the SSCs in mammals, which are supported by Sertoli cells, the *Drosophila* GSCs are encysted and supported by the somatic cyst stem cells (CySCs). The GSCs and CySCs are anchored to a group of somatic cells called the hub. The hub and CySC cells serve as the GSC niche in *Drosophila* (Zoller and Schulz 2012), similar to the Leydig and Sertoli cells in mammals (Oatley and Brinster 2012). In addition, many molecular

© The Author 2017. Published by Oxford University Press. All rights reserved. For permissions, please e-mail: journals.permissions@oup.com

as well as physiological aspects of GSC maintenance and differentiation are conserved from flies to mammals. For instance, common signaling pathways, including BMP/TGF-β, Jak/Stat and EGFR signaling, play critical roles in stem cell maintenance in both systems (Kanatsu-Shinohara et al. 2005; Kawase et al. 2004; Leatherman and Dinardo 2010; Meng et al. 2000; Oatley et al. 2009; Shivdasani and Ingham 2003; Singh et al. 2016).

One important component of the stem cell niche is a special type of carbohydrate-modified proteins, heparan sulfate proteoglycans (HSPGs). HSPGs are involved in a variety of biological processes such as growth factor signaling, cell adhesion and enzymatic catalysis. These molecules serve as co-receptors for growth factor signaling, regulating the distribution and reception of secreted signaling factors, such as BMPs, Wnts, Hedgehog and FGFs, on the cell surface (Kirkpatrick and Selleck 2007; Nakato and Li 2016). Recent studies have indicated critical roles for HSPGs in the stem cell niche (Guo and Wang 2009; Hayashi et al. 2009; Pennetier et al. 2012; Takemura and Nakato 2017). In fact, many stem cell niche factors are known to be HS-dependent. We previously showed that HSPGs are required in niche cells to non-cell autonomously regulate GSC maintenance in the *Drosophila* ovary (Dejima et al. 2011; Hayashi et al. 2009). We also demonstrated that in the testis GSC niche, HS in the hub affects GSC numbers through control of GSC division orientation (Levings et al. 2016). In the current study, we demonstrate that loss of HS in the hub disrupts normal growth factor signaling in differentiating somatic and germline cells, leading to a stem cell tumor phenotype. Our finding indicates a novel non-autonomous role for niche HS in ensuring the integrity of the niche and preventing tumor formation.

Results

Loss of heparan sulfate in hub results in tumorous testes

In our previous study, to determine the role of HS in the male GSC niche, we examined the effect of RNAi knockdown of *sulfateless* (*sfl*) specifically in the hub of adult testes using *upd-Gal4* with *tub-Gal80^{ts}* (referred to as hub *sfl* RNAi, experimental design shown in Supplementary Figure 1) (Levings et al. 2016). *sfl* encodes the only *Drosophila* HS *N*-deacetylase/*N*-sulfotransferase, which catalyzes the first step of the HS modification process. Since this step is critical for subsequent modification steps, removal of *sfl* renders HS biologically inactive (Lin and Perrimon 1999). We showed that hub *sfl* RNAi led to an increase in the number of GSCs maintained at the niche due to a defect in centrosome anchoring in GSCs, which is critical for their proper asymmetric division. Thus, loss of hub HS increases the rate of symmetric GSC divisions (Levings et al. 2016).

In addition to this effect of hub *sfl* RNAi on the asymmetric division of GSCs, we found that a fraction of testes (approximately 10%) showed abnormalities in gross morphology, such as a widened and blunted apical tip (Figure 1A and B, Table I) (Fuller 1993). Of these abnormal hub *sfl* RNAi testes, a few developed a more severe "tumorous" phenotype (approximately 5% of all hub *sfl* RNAi testes; Figure 1C). Furthermore, hub *sfl* RNAi testes showed abnormalities in the distinct, progressive organization of spermatogenic cells. In wild-type, more undifferentiated cell types are found closer to the niche and differentiated cells are found distally from the hub, as viewed by phase contrast microscopy (Figure 1A′ and A″). Conversely, in the tumorous hub *sfl* RNAi samples, a chaotic intermixing of germline cells from various stages of spermatogenesis was observed (Figure 1B′ and B″). In control testes

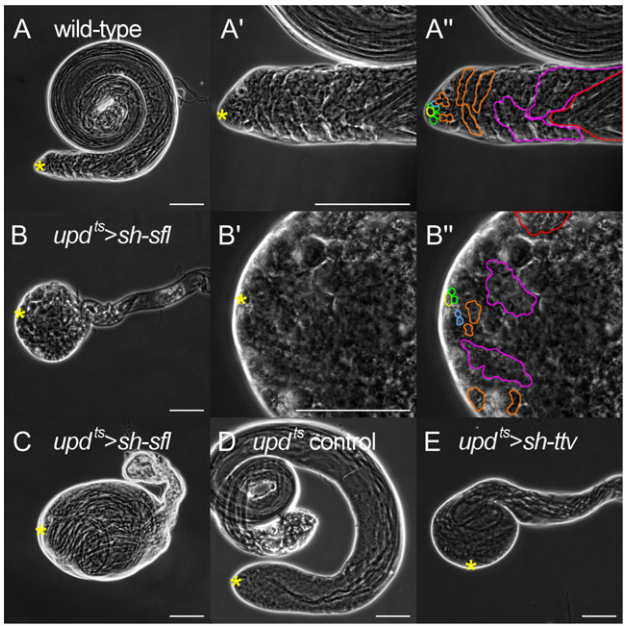

Fig. 1. Loss of hub HS results in tumorous testes and disrupts organization of spermatogenic cells. Phase contrast images of testes from wild-type (**A**–**A″**), *upd^{ts} > sh-sfl* (**B**–**C**), *upd^{ts}* control (**D**) and *upd^{ts} > sh-ttv* (**E**). **A′**–**A″** and **B′**–**B″** are high magnification views of **A** and **B**, respectively, showing organization of spermatogenic cells. To illustrate the progressive stages of differentiation as cells transit the testis, a few clearly identified examples of germline cell clusters at different stages of spermatogenesis are highlighted by outline color in **A″** and **B″**: yellow, hub; green, GSCs; blue, gonialblasts; orange, spermatogonia; pink, primary spermatocytes; red, elongating spermatids. The cells in wild-type advance through each stage of spermatogenesis in a successive, linear fashion from the testis tip distally. In *upd^{ts} > sh-sfl* testes, however, at least a portion of cells do not follow this normal, linear organization of differentiating cells. Severe "tumorous" phenotypes are seen in hub *sfl* RNAi (**B** and **C**) and hub *ttv* RNAi (**E**) testes. Yellow asterisks indicate hub location. Bars: 100 μm.

(*upd-Gal4*; *tub-Gal80^{ts}/{CaryP}attP2*), we observed no change in overall morphology and cell-type organization (Figure 1D), and no tumorous testes (Table I).

To confirm that the hub *sfl* RNAi phenotype is due to loss of HS activity, we tested the effect of knockdown of another HS biosynthetic enzyme, *tout velu* (*ttv*). *ttv* encodes an HS co-polymerase (Bellaiche et al. 1998) and HS is not biochemically detectable in *ttv* homozygous mutant larvae (Toyoda et al. 2000). We found that hub-specific knockdown of *ttv* showed phenotypes indistinguishable from hub *sfl* RNAi (Figure 1E), consistent with the idea that these phenotypes indeed result from compromised HS biosynthesis in the hub.

We next examined the effects of HS loss in different cell types of testes. We used *nanos-Gal4* and *c587-Gal4* to abrogate *sfl* in GSCs/germline cells and the somatic CySCs/cyst cells (CCs), respectively. None of these genotypes caused tumorous phenotypes or abnormal morphology (Supplementary Figure 2A and B). Thus, loss of HS specifically in the hub can cause widespread changes in both morphology and cell-type organization, which are associated with a germline tumor phenotype.

Hub *sfl* RNAi testes exhibit disrupted differentiation of germline cells

The observed disruption of cell-type organization in hub *sfl* RNAi suggested a defect in differentiation of GSCs/gonialblasts (GBs).

Table I. Ectopic stem cell frequency

Genotype	*N*	No ectopic SC	Ectopic CySC	Ectopic GSC	Any ectopic SC
upd^{ts} control	71	71	0	0	0
upd^{ts} > *sh-sfl*	88	79	5 (*)	8 (**)	9 (**)

Quantification of the number of testes containing: 1) no ectopic stem cells, 2) ectopic CySCs, 3) ectopic GSCs, 4) ectopic GSCs and/or ectopic CySCs. $^{*}P < 0.05$; $^{**}P < 0.01$. *N*: number of testes assayed.

Therefore, we tracked the differentiation status of these germline cell populations in hub *sfl* RNAi testes. Anti-Vasa (Vas) antibody staining in control testes showed concentrated signals in undifferentiated spermatogonia/GSCs (Figure 2A) (Bunt and Hime 2004; Kiger et al. 2000). Further distally, the Vas signal intensity gradually diminishes as the cells grow in size and mature through spermatogenesis. On the other hand, hub *sfl* RNAi testes showed several clusters of highly Vas-stained germline cells, which resembled undifferentiated spermatogonia/GSCs, quite distal to the germinal proliferation center (Figure 2B) (White-Cooper 2010). In addition, these cells showed the concentrated DNA staining characteristic of early germline cells (Figure 2C and D) (White-Cooper 2004). Thus, cells with several attributes indicating GSC/GB identity are found in abnormal locations distant from the hub (Table I).

Previous studies showed that overexpression of Dpp in germline cells caused overproliferation of partially differentiated germline cells (Bunt and Hime 2004; Parrott et al. 2012). Several aspects of the hub *sfl* RNAi phenotype were distinct from this Dpp overexpression. First, unlike the Dpp-induced event, the undifferentiated germline cells in hub *sfl* RNAi testes always lacked expression of Bam, a marker of differentiation detected in spermatogonia just before their transition to the spermatocyte stage (Figure 2F and F′) (Gonczy et al. 1997). Second, many of these cells lacked the fusomes of differentiating spermatogonia shown by branched Hu-li tai-shao (Hts) staining (examples of wild-type fusomes in Figure 2G). Instead, hub *sfl* RNAi testes exhibited the round Hts staining of the spectrosome normally observed in GSCs/GBs (Figure 2H). Based on these observations, we termed these undifferentiated germline cells, found distant from the niche in hub *sfl* RNAi testes, "ectopic GSCs".

Hub-specific *sfl* RNAi disrupts somatic cell differentiation

In the *Drosophila* testis, the development of germline and somatic cells is tightly coupled via communication between these cell populations (Sarkar et al. 2007; Singh et al. 2016; Smendziuk et al. 2015). We therefore analyzed the differentiation status of somatic cells in hub *sfl* RNAi testes by staining for Zfh-1 (a marker for undifferentiated CySCs) and Eyes absent (Eya; a marker for differentiated CCs). In control testes, CySCs are highly positive for Zfh-1 and differentiating CCs lose Zfh-1 signal within a few cell diameters away from the hub (Figure 2I) (Leatherman and Dinardo 2008). The Eya level increases simultaneously at this distance (Figure 2I) (Leatherman and Dinardo 2008). Hub *sfl* RNAi testes showed an altered distribution of these markers. Specifically, the range over which Zfh-1-positive CySCs/CCs are found adjacent the hub was significantly expanded (Figure 2J; Table II). In addition, populations of Zfh-1 positive, Eya-negative cells were sometimes detected very distant (>100 μM) from the niche, suggesting the presence of ectopic CySCs in hub *sfl* RNAi testes (Figure 2J).

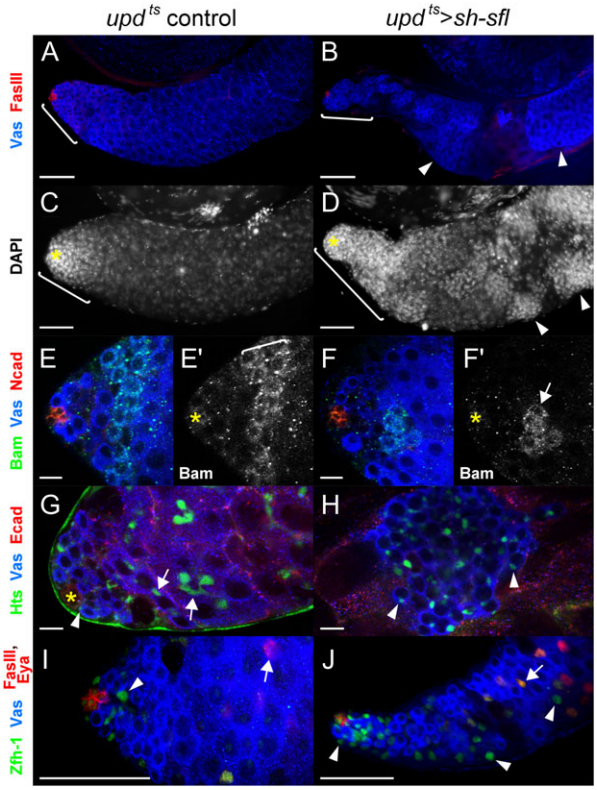

Fig. 2. Molecular characterization of tumorous hub *sfl* RNAi testis. Control (**A**, **C**, **E**, **G** and **I**) and hub *sfl* RNAi (**B**, **D**, **F**, **H** and **J**) were stained for Vas (**A**, **B**, **E**, **F**, **G**, **H**, **I** and **J**), DAPI (**C** and **D**), Bam (**E** and **F**), Hts (**G** and **H**), Zfh-1 (**I** and **J**) and Eya (**I** and **J**). The zone of early germline cells contains highly Vas- (**A**) and DAPI- (**C**) positive cells (bracket). In hub *sfl* RNAi, additional regions also show these features, which are indicative of an undifferentiated state (arrowheads in **B** and **D**). Bam is expressed in a stripe of mitotic spermatogonia 3–4 cell widths from the hub in control (bracket in **E′**). In hub *sfl* RNAi, Bam is absent in all but a few cells (arrow in **F′**). Hts staining marks round spectrosomes in GSCs (arrowheads in **G** and **H**), and dumb-bell or branched fusomes in differentiating germline cells (arrows) in control (**G**). In germline cells found distant from the niche in hub *sfl* RNAi, many cells have a spectrosome (arrowheads in **H**). Zfh-1 marks undifferentiated CySCs (arrowheads in **I** and **J**), while loss of Zfh-1 and increase in Eya intensity marks differentiating CCs (arrows in **I** and **J**). The hub was marked by antibodies against FasIII (**A**, **B**, **I** and **J**), N-cad (**E**–**F′**), or E-cad (**G** and **H**). Bars: 50 μm (**A**–**D**, **I** and **J**), 10 μm (**E**–**H**).

Table II. Zfh-1 range data

Genotype	*N*	Mean Zfh-1 range (μm)
upd^{ts} control	41	52.9
upd^{ts} > *sh-sfl*	48	64.4 (n.s.)
upd^{ts} > *sh-sfl* (testes with ectopic CySC)	4	208.0 (*)

Quantification of Zfh-1 intensity and range data. The mean Zfh-1 range was calculated using the assay described in Materials and Methods. n.s.: not significant; $^{*}P < 0.05$; *N*: number of testes assayed.

To quantify the range of Zfh-1-positive cells, we measured the distance between the hub and the Zfh-1-positive cell farthest from the hub (we term this the "Zfh-1 range") and averaged this value across all testes of a given genotype (Table II; see the Material and

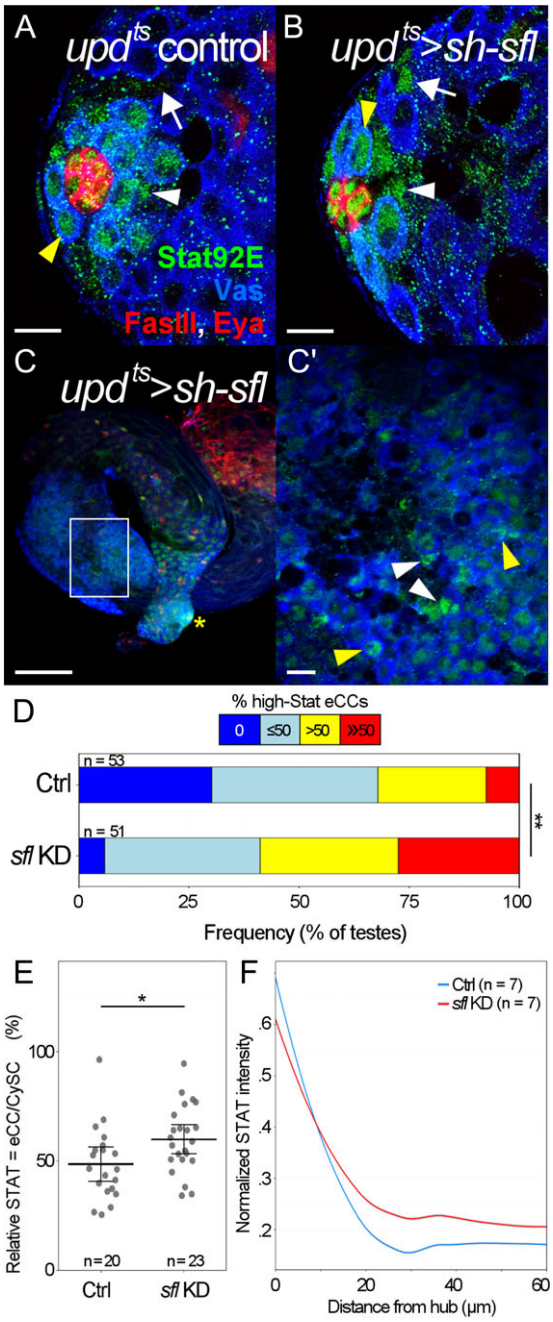

Fig. 3. Ectopic Jak/Stat activation in hub *sfl* RNAi. (**A**–**C**′) Anti-Stat antibody staining of control (**A**) and hub *sfl* RNAi (**B**–**C**′) testes. In control, strong nuclear Stat is detected in GSCs (yellow arrowhead) and CySCs (white arrowhead) (**A**). Stat signal is rapidly lost in eCCs (arrow). In hub *sfl* RNAi testes, strong Stat is seen in some eCCs as well (**B**). Ectopic stem cells (white rectangle) in hub *sfl* RNAi are found distant from the niche (yellow asterisk; **C**). A magnified image of the region enclosed by the rectangle shows population of cells with varying Jak/Stat signal, including potential ectopic GSCs and CySCs (**C**′). Additional antibodies used in panels **A**–**C**′ were directed against: FasIII, Vas and Eya. (**D**–**F**) Quantification of Jak/Stat signaling. (**D**) A significantly larger proportion of hub *sfl* RNAi testes had more eCCs with high-Stat signal than with low-Stat signal. It is important to note that, while ~25% of hub sfl RNAi testes contained eCCs with especially high Jak/Stat signaling, not all of these necessarily trigger true ectopic stem cell renewal events. It is possible that the Jak/Stat signal in these eCCs may need to be exceptionally high, or that other molecular events are necessary in concert with this amplified signal, to trigger such ectopic renewal. (**E**) Hub *sfl* RNAi eCCs have a Stat signal significantly closer to CySCs than control eCCs. (**F**) A normalized Stat signal gradient was drawn using the procedure described in Materials and Methods. Hub *sfl* RNAi shows a longer and shallower gradient, indicating that the ectopic Stat signaling could be caused by additional Jak/Stat ligand, Upd, distributed outside the niche. Numerical figures depict the mean ± SE. $*P < 0.05$; $**P < 0.01$. *n*: number of testes assayed. Bars: 10 µm (**A**–**B**, **C**′), 100 µm (**C**).

Methods section). The average Zfh-1 range in hub *sfl* RNAi samples containing stem cell tumors was significantly larger than in the control (Table II, $P = 0.018$). However, when the average Zfh-1 range of all hub *sfl* RNAi samples was compared to the control, this difference was not statistically significant due to the low penetrance of tumor formation in this genotype (Table II). Thus, loss of HS in the hub resulted in a stochastic expansion of the zone in which the population of undifferentiated somatic cells reside. Together, these results are congruous with our finding of ectopic GSCs in hub *sfl* RNAi samples, indicating that populations of both ectopic germline and somatic stem cells are found in these testes.

Our finding suggests that niche HS contributes to the hub's ability to restrict stem cell maintenance to the niche microenvironment. Previous studies have shown that CySCs/CCs play a role in triggering the differentiation of GSCs/gonialblasts (Hudson et al. 2013; Schulz et al. 2002). For instance, genetic ablation of CySCs and CCs can produce ectopic GSCs (Lim and Fuller 2012). These previous findings, together with our observations, suggest that the failure in restricting GSC and CySC renewal to the *sfl* RNAi hub could be due to a defect in CySC-to-CC differentiation.

Hub-specific *sfl* RNAi disrupted normal pattern of Jak/Stat signaling in the GSC/CySC niche

To explore the molecular basis of the hub *sfl* RNAi testis phenotypes, we asked if loss of HS in the hub affects niche signaling. Jak/Stat signaling is the primary pathway necessary for CySC maintenance (Leatherman and Dinardo 2010). Overexpression of Unpaired (Upd), a ligand of the Jak/Stat pathway, in germline cells using *nanos-Gal4* produces ectopic populations of both CySCs and (non-autonomously) GSCs (Leatherman and Dinardo 2008; Parrott et al. 2012). Although considerably less severe, the phenotype in hub *sfl* RNAi testes of ectopic CySC and GSC renewal is reminiscent of this Upd overexpression result. Furthermore, we previously demonstrated that Upd is an HS-dependent factor, which requires HS for normal signaling and distribution (Hayashi et al. 2012). We therefore monitored Jak/Stat signaling in hub *sfl* RNAi testes.

We first investigated whether the patterns of Jak/Stat activation in the hub *sfl* RNAi testis were altered using an antibody against Stat92E (aka Stat), a downstream target of Jak/Stat signaling in *Drosophila* (Chen et al. 2014). By visual examination, the levels of nuclear Stat in CySCs and GSCs were comparable between control and hub *sfl* RNAi (CySCs, white arrowheads; GSCs, yellow arrowheads; Figure 3A and B, Supplementary Figure 3A). However, we found that Stat levels in ectopic GSC and CySC populations in the hub *sfl* RNAi testes were highly variable, with a handful of cells showing significant Jak/Stat signal (Figure 3C and C′). We also noticed a difference in CCs just entering differentiation and not yet expressing appreciable levels of Eya, which are termed early stage cyst cells (eCCs) (Zoller and Schulz 2012). In hub *sfl* RNAi testes, eCCs tended to show elevated Stat levels compared to the control (arrow; Figure 3B) but there was variation in Stat levels in this

population. We therefore counted the number of eCCs with low or high levels of Stat expression in each testis (Figure 3D; see Materials and Methods). We found that a significantly larger percentage of hub *sfl* RNAi testes had more high-Stat than low-Stat eCCs (>50% high-Stat). In addition, a larger proportion of these testes showed at least one eCC with Stat intensity equal to or higher than in CySCs. These eCCs with especially high-Stat signal are likely ectopically renewing CySCs.

To more precisely characterize Jak/Stat signaling in hub *sfl* RNAi testes, we quantified the Stat signal in a variety of cell types. Since antibody staining can vary across sample sets, we compared the relative staining intensities between different cell types within each testis. Using this method, we were able to quantify the change in Jak/Stat signaling between CySCs at the hub and differentiating CCs distal to the hub, while simultaneously controlling for inter-sample variation in Stat staining. As expected, the ratio in Stat intensity between Eya-positive, differentiating CCs and CySCs was comparable between control and hub *sfl* RNAi (Supplementary Figure 3B). However, we found a statistically significant increase in the Stat ratio between Eya-negative eCCs and CySCs in hub *sfl* RNAi samples (Figure 3E).

Since HS functions to tether HS-binding ligands, loss of HS in the ligand-expressing cells could result in altered distribution of these ligands at the receiving cells (Matsumoto et al. 2010). In fact, HS has been previously found to regulate SSC maintenance by changing the distribution of GDNF ligand in mice (Langsdorf et al. 2011). Although we attempted to visualize the distribution of Upd ligand in testes, the currently available genetic tools and detection techniques made it difficult to directly determine the ligand's gradient patterns in this organ (data not shown). Jak/Stat "signaling gradients" regulating cell fate decisions have been previously described in other organs, such as *Drosophila* ovary (Hayashi et al. 2012; Xi et al. 2003). We therefore measured the overall change in the Jak/Stat signaling gradient from the apical tip, where the stem cell niche resides, to a distal region of the testes. We found that the rate of Jak/Stat signal loss as distance from the niche increases was dramatically reduced in hub *sfl* RNAi testes (Figure 3F). In addition, hub *sfl* RNAi resulted in a much higher basal level of Jak/Stat activity in cells distant from the niche. Together with our Stat ratio experiment, these results indicate that, despite the low penetrance of our ectopic stem cell phenotype, there was a significant increase in the activity of the main pathway responsible for CySC renewal (Jak/Stat) outside the normal zone of CySC maintenance.

Another pathway known to regulate multiple steps in somatic cell differentiation is the EGFR pathway (Hudson et al. 2013; Sarkar et al. 2007). This pathway, functioning in a coordinated fashion with Jak/Stat signaling, tightly regulates somatic cell fate in the testis (Singh et al. 2016). To examine the possible involvement of EGFR signaling in the phenotypes caused by hub *sfl* RNAi, we examined genetic interactions between *Egfr* and hub *sfl* RNAi. We found that a reduction of *Egfr* enhances the somatic cell differentiation defect of hub *sfl* RNAi testes, further slowing the differentiation process in CCs (Figure 4). This result supports our model that defective somatic cell differentiation is a fundamental factor driving hub *sfl* RNAi phenotypes. On the other hand, we did not detect a difference in the rate of tumor formation by deleting one copy of *Egfr* (data not shown). EGFR signaling regulates multiple steps of somatic cell differentiation, and previous studies have indicated that differing levels of EGFR signal may be required each of these steps (Hudson et al. 2013). Thus, it is not surprising that EGFR disruption influences some of the phenotypes and not others.

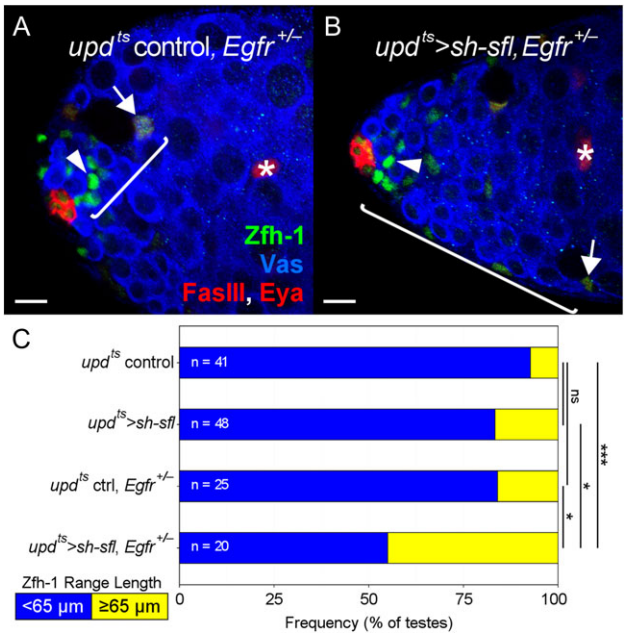

Fig. 4. Manipulation of somatic differentiation, using EGFR, shows genetic interaction with hub *sfl* RNAi phenotypes. (**A**–**B**) Effects of a loss of one copy of the Egfr ($Egfr^{+/-}$) on hub *sfl* RNAi CC differentiation. Control (**A**) and upd^{ts} > *sh-sfl*, (**B**) $Egfr^{+/-}$ testes samples were stained for Zfh-1 and Eya. Changes in the distance over which CCs differentiate were determined by measuring the Zfh-1 range, using the assay described in Materials and Methods. This range includes CySCs (arrowheads) and Zfh-1^+ differentiating CCs (arrows), but not Zfh-1^-, Eya^+ differentiated CCs (asterisks). The Zfh-1 range length is shorter in upd^{ts} control, $Egfr^{+/-}$ (bracket; **A**) as compared to upd^{ts} > *sh-sfl*, $Egfr^{+/-}$ (**B**). (**C**) Categorization of Zfh-1 range described in detail in the Materials and Methods. We found that upd^{ts} > *sh-sfl*, $Egfr^{+/-}$ had a significantly higher proportion of testes with a long Zfh-1 range length. Additional antibodies used in panels **A**–**C**′ were directed against: FasIII, a hub cell marker; and Vas, a germline cell marker. ns: not significant; $*P < 0.05$; $***P < 0.001$. *n*: number of testes assayed. Bars: 10 µm.

Discussion

Although retaining a pool of actively proliferating stem cells in close proximity to the local niche is an important physiological process in preventing cancer, the mechanism for how this is achieved is not well understood. Using the *Drosophila* male germline stem cell niche model, our study reveals that RNAi knockdown of *sfl*, an essential gene for HS biosynthesis, specifically in the hub leads to tumor formation. Hub *sfl* RNAi testes also lose the stereotypically ordered, progressive organization of spermatogenic cells that is conventionally observed in the testis. Instead, they produce groups of intermixed cells from various stages of spermatogenesis. The same phenotypes were reproduced by hub-specific knockdown of *ttv*, another critical HS biosynthetic gene, confirming that these phenotypes are caused by loss of functional HS in the hub.

How does the loss of HS in the hub modulate signal transduction in the environment around the niche? It has been shown that HSPGs play critical roles not only in signal reception but also ligand distribution in a tissue (Fujise et al. 2003; Hayashi et al. 2012; Koziel et al. 2004; Ohkawara et al. 2002; Takei et al. 2004). A recent study also suggested that the release of Sonic hedgehog from expressing cells is controlled by HS, which affects its signaling in receiving cells (Ortmann et al. 2015). Thus, hub HS could affect the

level of an HS-dependent, hub-derived ligand at the niche, thereby modulating signaling in the receiving cells. We propose that hub HS normally limits the signal range of the ligand Upd to contacting stem cell populations, predominantly (Figure 5A). When hub HS is lost, Upd acts in more distant locations, triggering ectopic Jak/Stat signaling and stem cell renewal events (Figure 5B).

The phenotypes of hub *sfl* RNAi testes were observed at relatively low frequencies: gross morphological defects and tumor formation were seen in approximately 10% and 5% of all hub *sfl* RNAi testes, respectively. Several lines of evidence indicate that this is not due to the low efficiency of knockdown. The identical *UAS-sh-sfl* strain has been used in previous studies by us and others in which it induced various phenotypes at much higher penetrance in different contexts (Levings et al. 2016; Zhang et al. 2013). When expressed in the wing disc, it disrupts Dpp- and Wg-dependent patterning processes at 100% penetrance, mimicking a *sfl* null mutation (unpublished data). Thus, the morphological defects and tumor formation in hub *sfl* RNAi testes are more likely to be true low penetrance events rather than a result of low knockdown efficiency.

In previous studies, Upd overexpression resulted in massive overproliferation of CySCs along with associated ectopic GSCs (Leatherman and Dinardo 2008). We found that hub *sfl* RNAi led to a more moderate phenotype with sporadic cells expressing ectopically high levels of Stat (Figure 3B), instead of overall and uniform increase of signaling. This makes sense, since we did not manipulate the overall levels of Upd ligand in testes and thus the additional ligand outside the niche would be minor relative to previous Upd overexpression experiments. Interestingly, overall tissue morphology as well as markers of germline differentiation, such as Vas, Bam and Hts, appeared normal in the majority of hub *sfl* RNAi testes (hence the low penetrance of tumor phenotype). In comparison, Jak/Stat signaling was moderately but significantly affected across all hub *sfl* RNAi testes. Thus, it is likely that only the testes with the most severe alteration of Jak/Stat signaling result in disruption of these other germline markers and an eventual tumorous phenotype. It is also possible that other molecular events may be necessary in addition to altered Jak/Stat signaling to induce the tumorous phenotype. Together, even if functional HS is consistently removed from the hub, the formation of germline and somatic tumors is a stochastic event. This is somewhat similar to cancer formation in mammals, where individuals with certain genetic variants are more susceptible to oncogenesis, yet not guaranteed to acquire cancer in their lifetime.

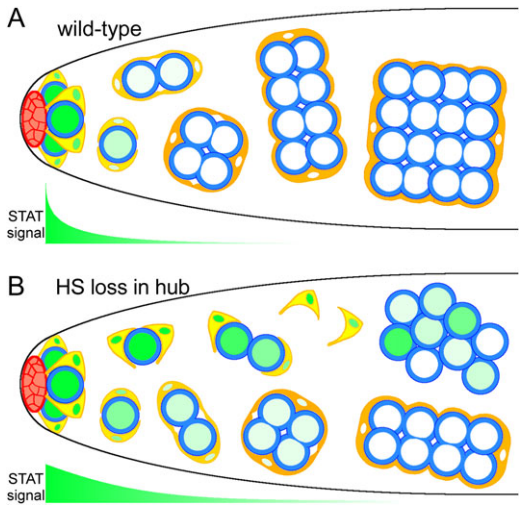

Fig. 5. Model - ectopic Jak/Stat signaling sporadically prevents CySC differentiation. A diagram showing a model for the role of HS in Upd/Stat signal distribution. (**A**) In wild-type, HS on the hub retains the majority of Upd ligand at the niche. Only CySCs (yellow) and GSCs (single blue cells) that contact the hub receive sufficient Jak/Stat signaling (green) to be renewed as stem cells. (**B**) When HS is lost, the Upd/Stat signaling range is expanded, resulting in stochastic ectopic renewal of cyst cell daughters as CySCs. This decouples the differentiation of CCs and germline cells, which leads to ectopic populations of stem cells.

The fact that disruption of HS biosynthesis in the hub predisposes flies to germline tumor formation recapitulates several aspects of the niche-driven model of mammalian cancer formation previously discussed (Radisky and Bissell 2004). First, a certain signaling pathway, with directionality from stromal/niche cells to downstream tissue cells, is responsible for normal tissue function and suppressing tumor formation. Second, a defect or mutation in the stromal/niche cells can nonautonomously lead to tumor formation in adjacent cell populations. Given that the cellular and molecular basis for GSC maintenance and differentiation is well conserved between flies and mammals, it is possible that aberrant HS in the niche may be one molecular event leading to human testicular germ cell tumors. This *Drosophila* model, in which HS structures are altered in the hub, can offer a useful system to gain further insights into molecular pathways involved in human germline tumors as well as new possible therapies for treatment.

Materials and Methods

Fly strains

Detailed information for the fly strains used is described in Flybase (http://flybase.bio.indiana.edu/) except where noted. The wild-type strain used was Oregon R. Other strains used were: *unpaired* (*upd*)-*Gal4* (Halder et al. 1995); *nanos* (*nos*)-*Gal4 VP16* (Van Doren et al. 1998); *c587-Gal4* (Kai and Spradling 2003); *tubulin* (*tub*)-*Gal80^{ts}* (McGuire et al. 2003); *UAS-sh-sfl*, a UAS short-hairpin RNAi strain for *sfl* (Zhang et al. 2013); *UAS-sh-ttv*, a UAS short-hairpin RNAi strain for *ttv*; *P{CaryP}attP2*, an isogenic parent strain used for targeted insertion of TRiP short-hairpin constructs into the attP2 locus; *Egfr^{1K35}*, a null allele of the EGF receptor (Nüsslein-Volhard et al. 1984; Raz et al. 1991).

The TARGET (Gal4-Gal80^{ts}) system was used to induce *UAS-sh-sfl* expression in specific cell types of the adult testis (Kleinschmit et al. 2013; McGuire et al. 2003). For hub cell-specific knockdown, animals with the genotype of *upd-Gal4*; *tub-Gal80^{ts}/UAS-sh-sfl* were raised at the Gal80^{ts} permissive temperature (18°C). Adult flies were transferred to a new vial at 0–6 days after eclosion, the temperature was shifted to the Gal80^{ts} restrictive temperature (30°C) and they were incubated for an additional 10 days (diagram of experimental scheme in Supplementary Figure 1). Flies were transferred to fresh food at least once every 2 days. *nos-Gal4 VP16* and *c587-Gal4* (along with *tub-Gal80^{ts}*) were used for germline cell- and the CySC/CC-specific expression, respectively. The control strains used in each of these RNAi experiments were generated by crossing the respective Gal4 TARGET strain with the isogenic parent strain of the TRiP lines, *P{CaryP}attP2*. For example, hub RNAi control flies had the genotype *upd-Gal4*; *tub-Gal80^{ts}/P{CaryP}attP2*.

Immunofluorescence staining

Immunostaining was performed as previously described (Dejima et al. 2013; Fujise et al. 2001; Salzmann et al. 2013). In short,

samples were fixed for 30 min with 4% formaldehyde in PBS, permeabilized in 0.3% PBST (0.3% Triton X-100 in PBS) for 20 min (10 min, twice) and washed with 0.1% PBST (10 min, twice). They were then blocked in 5% normal goat serum in 0.1% PBST for 1 h, and incubated overnight in primary antibodies at 4°C. Samples were again washed in 0.1% PBST (10 min, three times) and incubated with the appropriate AlexaFluor secondary antibodies either overnight at 4°C or for 2 h at room temperature. Next, they were washed in 0.1% PBST (10 min, four times), before being mounted in VECTASHIELD (H-1000 or H-1200, Vector Laboratory). Images were obtained using either a Zeiss 710 or a Nikon Eclipse E800 laser scanning confocal microscope.

The following primary antibodies were used: rabbit anti-Vas (1:500, a gift from S. Kobayashi), chick anti-Vas (1:1000, a gift from S. Kobayashi), mouse anti-Hu-li tai-shao (Hts) (1:5, Developmental Studies Hybridoma Bank), mouse anti-Bam (1:30, DSHB), rabbit anti-Zfh-1 (1:5000, a gift from R. Lehmann), rat anti-E-cadherin (E-cad; 1:40, DSHB), rat anti-N-cadherin (N-cad; 1:20, DSHB), mouse anti-FasciclinIII (FasIII; 1:200, DSHB), mouse anti-Eya (1:30, DSHB) and rabbit anti-Stat92E (1:5000, a gift from Y. Hayashi). Secondary antibodies were from the AlexaFluor series (1:500; Molecular Probes).

Frequency scoring of ectopic stem cells

To score the rate of ectopic stem cell frequency in testes of different genotypes (recorded in Table I), we stained testes with antibodies that mark the hub (anti-FasIII), germline cells (anti-Vas) and DAPI. Most samples were also stained with an antibody that marks CySCs (anti-Zfh-1). To count the number of testes with ectopic stem cells, we scanned through the full depth of samples using either a Nikon Eclipse E800 laser scanning confocal microscope or a Zeiss AxioSkop 2 epifluorescence microscope. The DAPI channel was first used to grossly scan for any tumor phenotype, then the samples were more thoroughly inspected by examining Vas and Zfh-1 staining. Samples were considered to be positive for GSC tumors when clusters of germline cells that were small (~7 μm wide) and highly Vas-stained were detected greater than ~100 μm from the hub (frequently, these undifferentiated cells were found among more differentiated germline cells such as primary spermatocytes or later stages). Samples were considered to be positive for CySC tumors when multiple Zfh-1 positive somatic cells were detected greater than ~100 μm from the hub. To calculate the rate of ectopic stem cell tumors, the number of testes with both GSC and/or CySC tumors were tallied. We divided the total number of testes containing any of these stem cell tumors by the total number of testes examined for each genotype to obtain the stem cell tumor frequency.

Quantification of cell-specific Stat signal and gradient

To assay changes in Jak/Stat signaling in different cell types of the testis, we stained them with antibodies against the hub (anti-FasIII), germline (anti-Vas), differentiating cyst cells (anti-Eya), Stat92E and DAPI as a nuclear marker. We used a confocal microscope to take images of a single plane of each testis in which the hub, as well as several GSCs and CySCs, were transected. We used Fiji's ROI Manager and Measure functions to measure the mean nuclear Stat signal for 2–3 cells of each of the following cell types per testis (example cells are shown in Figure 3): 1) GSCs (yellow arrowheads), 2) CySCs (white arrowheads), 3) early stage cyst cells (eCCs, white arrows) and 4) Eya-positive cyst cells. To quantify Jak/Stat signaling level, a line (10-pixels wide) was drawn within the nucleus (using the DAPI channel) of each cell, and then the average signal intensity was measured on the Stat channel. Quantification of nuclear Stat signal has been previously established as a readout for Jak/Stat signaling levels (Chen et al. 2014; Xi et al. 2003). These Stat intensity values were recorded in Microsoft Excel, and calculations of mean Stat intensity for each cell type, within *each* testis, were computed in *R*. Comparisons of relative Stat intensity (such as in Figure 3E) were calculated in *R* by dividing the mean Stat intensity for one cell type by the mean Stat intensity of another cell type in a pair-wise fashion for *each* testis sample, which gave us the relative Stat ratio. We used these relative Stat ratios from each testis to compute the average Stat ratio of each genotype and for the accompanying statistical tests.

To generate the Stat gradients shown in Figure 3F, we used Fiji and *R* to analyze confocal sections of testes. In this analysis, we used Fiji's ROI Manager to draw seven equally spaced, radiating lines (each 10-pixels wide) from an intersecting point in the very center of the hub, which extended approximately 50–70 μm distally into the testis. We excluded Stat signal within the hub by shortening the lines to begin at the interface between GSCs and the hub. Next, we used Fiji's Multi-Plot function to plot distance (*X*)-to-intensity (*Y*) profiles of the Stat signal for seven testes of each genotype (each containing profiles for seven radiating lines). We recorded these values in Microsoft Excel and then imported the data into *R*. In *R*, we normalized the intensities using the following methodology. First, we obtained the maximum Stat intensity value from each of the seven linetraces per testis, and calculated an average-maximum Stat intensity for each testis. We normalized the data by dividing all the absolute Stat intensity values (for each data point of each linetrace profile) by the average-maximum Stat value corresponding to the testis from which the Stat intensity data was taken. This provided the normalized Stat values for all linetrace profiles. Using the pixel distance (in μm) as the *X* values, and the normalized Stat intensity as the *Y* values, we next plotted the data in *R* using the *ggplot2* package's "stat_smooth" function. We grouped samples according to genotype, and used the "loess" method to average across all 49 linetrace profiles (seven linetrace profiles for seven testes of each genotype) to draw an average normalized Stat intensity profile for each genotype.

Frequency scoring of ectopic Stat signal

To determine the frequency of testes containing significantly higher proportions of early stage cyst cells (eCCs) with high-Stat signal, pictured in Figure 3D, we stained testes with antibodies that mark the hub (anti-FasIII), germline cells (anti-Vas), differentiating cyst cells (anti-Eya), Jak/Stat signal (anti-Stat92E) and DAPI. We used a confocal microscope to take images of each testis using the same criteria as in the previous Stat signaling methodology, above. We then grouped both control and hub *sfl* RNAi samples, randomized and performed the following single-blind experiments (experimenter was blind to sample genotypes). We counted the total number of eCCs present (which were identified as $DAPI^+$, Vas^-, Eya^- cells found greater than 2–3 cell widths, or ~14 μm, from the hub). We compared the Stat levels in each eCC with the Stat levels in CySCs (which were identified by the same staining pattern, but found just outside GSCs and less than 14 μm from the hub). Stat levels in CySCs were typically quite high. The eCCs were classified into one of the following groups: 1) low-Stat, with a Stat signal approximately 50% or less than that of CySCs, 2) high-Stat, with a Stat signal between 50% and ~90% of the CySC signal and 3) "super"-Stat, with a Stat signal approximately equal to or higher than that in CySCs. After recording the number of each type of eCC in each

sample in Microsoft Excel and reassociating the sample IDs with their respective genotypes, we imported the data into *R* for the remaining steps. First, we calculated the percentage of eCCs in each testis that were either high-Stat or super-Stat ([high-Stat + super-Stat] ÷ [low-Stat + high-Stat + super-Stat]), and labeled this quantification as the percent high-Stat eCCs. We then categorized each testis into one of four categories: 1) contains 0 high-Stat eCCs, 2) contains 50% or less high-Stat eCCs, 3) contains more than 50% high-Stat eCCs but no super-Stat eCCs or 4) contains more than 50% high-Stat eCCs and at least one super-Stat eCC. We used *R* to count the number of testes in each group, for each genotype, and generated the graph in Figure 3D. We also used *R* for statistical tests on this categorical data (described in the Statistics subsection).

Quantification and categorization of "Zfh-1 range"

We assayed the length of the Zfh-1 range in testes as a way to investigate the distance over which CySCs differentiate into CCs. To measure these Zfh-1 range lengths, we stained testes with antibodies that mark the hub (anti-FasIII), germline cells (anti-Vas), CySCs (anti-Zfh-1) and differentiating cyst cells (CCs; anti-Eya). It has been previously found that CCs undergoing differentiation can still express appreciable levels of Zfh-1 several cell diameters from the hub (Monahan and Starz-Gaiano 2016; Zoller and Schulz 2012). As this Zfh-1 expression is rapidly lost during somatic differentiation, Eya expression is upregulated. We used a confocal microscope to scan through samples and obtained an image of each testis at a single Z-section/plane. The section was chosen when we could visualize both the hub and a single CC, still expressing appreciable levels of Zfh-1, found farthest from the hub. Using Fiji's Measure function, we quantified three values in each of these images: 1) the Zfh-1 range- i.e., the length (in μm) of a line drawn from the edge of the hub (on the side closest to the CC) to the center of this farthest Zfh-1 expressing somatic cell, 2) the mean Zfh-1 intensity of a line (10-pixels wide) drawn through an average CySC (examples in Figure 4, arrowheads) and 3) the mean Zfh-1 intensity of a line (10-pixels wide) drawn through the CC used for the length measurement (examples in Figure 4, arrows). These values were recorded in Microsoft Excel and used to compute the mean Zfh-1 range length and the mean CC-to-CySC Zfh-1 intensity ratio (which was calculated for each testis sample by dividing the Zfh-1 intensity values of the chosen CC by the chosen CySC) for each genotype in *R*. The mean Zfh-1 range values are shown in Table II, and there were no significant differences in Zfh-1 intensity ratio values (data not shown). The individual quantifications were used to assign testes of each genotype to different Zfh-1 range length categories, described in the next paragraph.

We imported the Zfh-1 range data into *R*, and used the control strains (*upd-Gal4*; *P{CaryP}attP2 / tub-Gal80^{ts}* and *upd-Gal4*; + / *Egfr^{1K35}*; + / *tub-Gal80^{ts}*) to calculate the mean Zfh-1 range and standard deviation for the controls. We added one respective standard deviation value to the mean Zfh-1 range for each control genotype to calculate the "normal" Zfh-1 range for each genotype. The average normal Zfh-1 range was between 0 and approximately 65 μm from the hub. The value of 65 μm was chosen as the cut-off between a "normal" and "long" Zfh-1 range because, based on the previous calculations of mean and standard deviations, it was expected that the majority of control testes (approximately 84%) would have a range of this length or less. We then used *R* to assign testes from each genotype to the appropriate Zfh-1 range length category, and generated the graph in Figure 4E. We also used *R* for statistical tests on this data (described in the Statistics subsection).

Statistics

R was used for all statistical calculations. A variation of two-tailed Student's *t*-test that assumes unequal sample variance, called Welch's *t*-test, was used to calculate *P*-values for Figure 3E, Supplementary Figure 3 and Table II. Chi-squared tests were used to calculate *P*-values for Figures 3D, 4C, and Table I. All experiments included two or more biological replicates.

Supplementary data

Supplementary data are available at *Glycobiology* online.

Acknowledgments

We are grateful to Y. Hayashi, S. Kobayashi, R. Lehmann, T. Neufeld, M. O'Connor, the Developmental Studies Hybridoma Bank, the Bloomington Stock Center, and TRiP at Harvard Medical School for fly stocks, reagents and equipment usage. We thank M. Takemura and T. Su for helpful discussions and critical reading of the manuscript.

Conflict of interest statement

None declared.

Abbreviations

CC, cyst cell; CySC, cyst stem cell; GB, gonialblast; GSC, germline stem cell; HS, heparan sulfate; HSPG, heparan sulfate proteoglycan; Sfl, Sulfateless; Upd, Unpaired.

Funding

This work was supported by a research grant from the National Institute of General Medical Sciences (R01GM115099).

References

Bellaiche Y, The I, Perrimon N. 1998. Tout-velu is a Drosophila homologue of the putative tumour suppressor EXT-1 and is needed for Hh diffusion. *Nature*. 394:85–88.

Bhowmick NA, Neilson EG, Moses HL. 2004. Stromal fibroblasts in cancer initiation and progression. *Nature*. 432:332–337.

Bunt SM, Hime GR. 2004. Ectopic activation of Dpp signalling in the male Drosophila germline inhibits germ cell differentiation. *Genesis*. 39:84–93.

Chen Q, Giedt M, Tang L, Harrison DA. 2014. Tools and methods for studying the Drosophila JAK/STAT pathway. *Methods*. 68:160–172.

Clarke MF, Fuller M. 2006. Stem cells and cancer: Two faces of eve. *Cell*. 124:1111–1115.

Dejima K, Kanai MI, Akiyama T, Levings DC, Nakato H. 2011. Novel contact-dependent bone morphogenetic protein (BMP) signaling mediated by heparan sulfate proteoglycans. *J Biol Chem*. 286:17103–17111.

Dejima K, Kleinschmit A, Takemura M, Choi PY, Kinoshita-Toyoda A, Toyoda H, Nakato H. 2013. The role of Drosophila heparan sulfate 6-o-endosulfatase in sulfation compensation. *J Biol Chem*. 288:6574–6582.

Fujise M, Izumi S, Selleck SB, Nakato H. 2001. Regulation of dally, an integral membrane proteoglycan, and its function during adult sensory organ formation of Drosophila. *Dev Biol*. 235:433–448.

Fujise M, Takeo S, Kamimura K, Matsuo T, Aigaki T, Izumi S, Nakato H. 2003. Dally regulates Dpp morphogen gradient formation in the Drosophila wing. *Development*. 130:1515–1522.

Fuller MT. 1993. Spermatogenesis. In: Bate M, Martinez-Arias A, editors. *The Development of* Drosophila melanogaster. Cold Spring Harbor (NY): Cold Spring Harbor Laboratory Press. p. 71–147.

Gilbert D, Rapley E, Shipley J. 2011. Testicular germ cell tumours: Predisposition genes and the male germ cell niche. *Nat Rev Cancer*. 11: 278–288.

Gonczy P, Matunis E, DiNardo S. 1997. bag-of-marbles and benign gonial cell neoplasm act in the germline to restrict proliferation during Drosophila spermatogenesis. *Development*. 124:4361–4371.

Guo Z, Wang Z. 2009. The glypican Dally is required in the niche for the maintenance of germline stem cells and short-range BMP signaling in the Drosophila ovary. *Development*. 136:3627–3635.

Hai Y, Hou J, Liu Y, Yang H, Li Z, He Z. 2014. The roles and regulation of Sertoli cells in fate determinations of spermatogonial stem cells and spermatogenesis. *Semin Cell Dev Biol*. 29:66–75.

Halder G, Callaerts P, Gehring WJ. 1995. Induction of ectopic eyes by targeted expression of the eyeless gene in Drosophila. *Science*. 267: 1788–1792.

Hayashi Y, Kobayashi S, Nakato H. 2009. Drosophila glypicans regulate the germline stem cell niche. *J Cell Biol*. 187:473–480.

Hayashi Y, Sexton TR, Dejima K, Perry DW, Takemura M, Kobayashi S, Nakato H, Harrison DA. 2012. Glypicans regulate JAK/STAT signaling and distribution of the Unpaired morphogen. *Development*. 139: 4162–4171.

Houghton J, Stoicov C, Nomura S, Rogers AB, Carlson J, Li H, Cai X, Fox JG, Goldenring JR, Wang TC. 2004. Gastric cancer originating from bone marrow-derived cells. *Science*. 306:1568–1571.

Hudson AG, Parrott BB, Qian Y, Schulz C. 2013. A temporal signature of epidermal growth factor signaling regulates the differentiation of germline cells in testes of Drosophila melanogaster. *PLoS ONE*. 8:e70678.

Kai T, Spradling A. 2003. An empty Drosophila stem cell niche reactivates the proliferation of ectopic cells. *Proc Natl Acad Sci USA*. 100: 4633–4638.

Kanatsu-Shinohara M, Miki H, Inoue K, Ogonuki N, Toyokuni S, Ogura A, Shinohara T. 2005. Long-term culture of mouse male germline stem cells under serum-or feeder-free conditions. *Biol Reprod*. 72:985–991.

Kawase E, Wong MD, Ding BC, Xie T. 2004. Gbb/Bmp signaling is essential for maintaining germline stem cells and for repressing bam transcription in the Drosophila testis. *Development*. 131:1365–1375.

Kiger AA, White-Cooper H, Fuller MT. 2000. Somatic support cells restrict germline stem cell self-renewal and promote differentiation. *Nature*. 407: 750–754.

Kirkpatrick CA, Selleck SB. 2007. Heparan sulfate proteoglycans at a glance. *J Cell Sci*. 120:1829–1832.

Kleinschmit A, Takemura M, Dejima K, Choi PY, Nakato H. 2013. Drosophila heparan sulfate 6-O-endosulfatase Sulf1 facilitates wingless (Wg) protein degradation. *J Biol Chem*. 288:5081–5089.

Koziel L, Kunath M, Kelly OG, Vortkamp A. 2004. Ext1-dependent heparan sulfate regulates the range of Ihh signaling during endochondral ossification. *Dev Cell*. 6:801–813.

Krausz C, Looijenga LH. 2008. Genetic aspects of testicular germ cell tumors. *Cell Cycle*. 7:3519–3524.

Krentz AD, Murphy MW, Kim S, Cook MS, Capel B, Zhu R, Matin A, Sarver AL, Parker KL, Griswold MD et al. 2009. The DM domain protein DMRT1 is a dose-sensitive regulator of fetal germ cell proliferation and pluripotency. *Proc Natl Acad Sci USA*. 106:22323–22328.

Langsdorf A, Schumacher V, Shi X, Tran T, Zaia J, Jain S, Taglienti M, Kreidberg JA, Fine A, Ai X. 2011. Expression regulation and function of heparan sulfate 6-O-endosulfatases in the spermatogonial stem cell niche. *Glycobiology*. 21:152–161.

Leatherman JL, Dinardo S. 2008. Zfh-1 controls somatic stem cell self-renewal in the Drosophila testis and nonautonomously influences germline stem cell self-renewal. *Cell Stem Cell*. 3:44–54.

Leatherman JL, Dinardo S. 2010. Germline self-renewal requires cyst stem cells and stat regulates niche adhesion in Drosophila testes. *Nat Cell Biol*. 12:806–811.

Levings DC, Arashiro T, Nakato H. 2016. Heparan sulfate regulates the number and centrosome positioning of Drosophila male germline stem cells. *Mol Biol Cell*. 27:888–896.

Lim JG, Fuller MT. 2012. Somatic cell lineage is required for differentiation and not maintenance of germline stem cells in Drosophila testes. *Proc Natl Acad Sci USA*. 109:18477–18481.

Lin X, Perrimon N. 1999. Dally cooperates with Drosophila Frizzled 2 to transduce Wingless signalling. *Nature*. 400:281–284.

Matsumoto Y, Matsumoto K, Irie F, Fukushi J, Stallcup WB, Yamaguchi Y. 2010. Conditional ablation of the heparan sulfate-synthesizing enzyme Ext1 leads to dysregulation of bone morphogenic protein signaling and severe skeletal defects. *J Biol Chem*. 285:19227–19234.

McGuire SE, Le PT, Osborn AJ, Matsumoto K, Davis RL. 2003. Spatiotemporal rescue of memory dysfunction in Drosophila. *Science*. 302:1765–1768.

Meng X, Lindahl M, Hyvonen ME, Parvinen M, de Rooij DG, Hess MW, Raatikainen-Ahokas A, Sainio K, Rauvala H, Lakso M et al. 2000. Regulation of cell fate decision of undifferentiated spermatogonia by GDNF. *Science*. 287:1489–1493.

Monahan AJ, Starz-Gaiano M. 2016. Apontic regulates somatic stem cell numbers in Drosophila testes. *BMC Dev Biol*. 16:5.

Nakato H, Li JP. 2016. Functions of heparan sulfate proteoglycans in development: Insights from Drosophila models. *Int Rev Cell Mol Biol*. 325:275–293.

Nüsslein-Volhard C, Wieschaus E, Kluding H. 1984. Mutations affecting the pattern of the larval cuticle in Drosophila melanogaster. *Wilhelm Roux's Arch Dev Biol*. 193:267–282.

Oatley JM, Brinster RL. 2012. The germline stem cell niche unit in mammalian testes. *Physiol Rev*. 92:577–595.

Oatley JM, Oatley MJ, Avarbock MR, Tobias JW, Brinster RL. 2009. Colony stimulating factor 1 is an extrinsic stimulator of mouse spermatogonial stem cell self-renewal. *Development*. 136:1191–1199.

Ohkawara B, Iemura S, ten Dijke P, Ueno N. 2002. Action range of BMP is defined by its N-terminal basic amino acid core. *Curr Biol*. 12:205–209.

Ortmann C, Pickhinke U, Exner S, Ohlig S, Lawrence R, Jboor H, Dreier R, Grobe K. 2015. Sonic hedgehog processing and release are regulated by glypican heparan sulfate proteoglycans. *J Cell Sci*. 128: 2374–2385.

Parrott BB, Hudson A, Brady R, Schulz C. 2012. Control of germline stem cell division frequency—a novel, developmentally regulated role for epidermal growth factor signaling. *PLoS ONE*. 7:e36460.

Pennetier D, Oyallon J, Morin-Poulard I, Dejean S, Vincent A, Crozatier M. 2012. Size control of the Drosophila hematopoietic niche by bone morphogenetic protein signaling reveals parallels with mammals. *Proc Natl Acad Sci USA*. 109:3389–3394.

Radisky DC, Bissell MJ. 2004. Cancer. Respect thy neighbor! *Science*. 303: 775–777.

Raz E, Schejter ED, Shilo BZ. 1991. Interallelic complementation among DER/flb alleles: Implications for the mechanism of signal transduction by receptor-tyrosine kinases. *Genetics*. 129:191–201.

Salzmann V, Inaba M, Cheng J, Yamashita YM. 2013. Lineage tracing quantification reveals symmetric stem cell division in Drosophila male germline stem cells. *Cell Mol Bioeng*. 6:441–448.

Sarkar A, Parikh N, Hearn SA, Fuller MT, Tazuke SI, Schulz C. 2007. Antagonistic roles of Rac and Rho in organizing the germ cell microenvironment. *Curr Biol*. 17:1253–1258.

Scadden DT. 2006. The stem-cell niche as an entity of action. *Nature*. 441: 1075–1079.

Schulz C, Wood CG, Jones DL, Tazuke SI, Fuller MT. 2002. Signaling from germ cells mediated by the rhomboid homolog stet organizes encapsulation by somatic support cells. *Development*. 129:4523–4534.

Shivdasani AA, Ingham PW. 2003. Regulation of stem cell maintenance and transit amplifying cell proliferation by tgf-beta signaling in Drosophila spermatogenesis. *Curr Biol*. 13:2065–2072.

Singh SR, Liu Y, Zhao J, Zeng X, Hou SX. 2016. The novel tumour suppressor Madm regulates stem cell competition in the Drosophila testis. *Nat Commun*. 7:10473.

Smendziuk CM, Messenberg A, Vogl AW, Tanentzapf G. 2015. Bidirectional gap junction-mediated soma-germline communication is essential for spermatogenesis. *Development*. 142:2598–2609.

Takei Y, Ozawa Y, Sato M, Watanabe A, Tabata T. 2004. Three Drosophila EXT genes shape morphogen gradients through synthesis of heparan sulfate proteoglycans. *Development*. 131:73–82.

Takemura M, Nakato H. 2017. Drosophila Sulf1 is required for the termination of intestinal stem cell division during regeneration. *J Cell Sci*. 130:332–343.

Toyoda H, Kinoshita-Toyoda A, Selleck SB. 2000. Structural analysis of glycosaminoglycans in Drosophila and Caenorhabditis elegans and demonstration that tout-velu, a Drosophila gene related to EXT tumor suppressors, affects heparan sulfate in vivo. *J Biol Chem*. 275:2269–2275.

Van Doren M, Williamson AL, Lehmann R. 1998. Regulation of zygotic gene expression in Drosophila primordial germ cells. *Curr Biol*. 8: 243–246.

White-Cooper H. 2004. Spermatogenesis: Analysis of meiosis and morphogenesis. In: Henderson D, editor. *Drosophila Cytogenetics Protocols*. Totowa, NJ: Humana Press. p. 45–75.

White-Cooper H. 2010. Molecular mechanisms of gene regulation during Drosophila spermatogenesis. *Reproduction*. 139:11–21.

Xi R, McGregor JR, Harrison DA. 2003. A gradient of JAK pathway activity patterns the anterior-posterior axis of the follicular epithelium. *Dev Cell*. 4:167–177.

Zhang Y, You J, Ren W, Lin X. 2013. Drosophila glypicans Dally and Dally-like are essential regulators for JAK/STAT signaling and Unpaired distribution in eye development. *Dev Biol*. 375:23–32.

Zoller R, Schulz C. 2012. The Drosophila cyst stem cell lineage: Partners behind the scenes? *Spermatogenesis*. 2:145–157.